Research Proposal

Improving Seismic Monitoring with Arrays of Three-Component Seismometers: Investigations Using a New Regional Array in Saudi Arabia and Three-Component Stations Throughout the Middle East

Lead Institution: University of Utah
Lead Principal Investigator: Dr. Keith Koper, University of Utah, Seismograph Stations, 115 S 1460 E, Salt Lake City, UT, 84112, USA, Tel. (801)-581-6274; kkoper@gmail.com

Team Organization 1: King Saud University
Principal Investigator of Team Organization 1: Dr. Abdullah Al Amri, Dept. of Geology, King Saud University, P.O. Box 2455, Riyadh, 11451, Saudi Arabia, Tel : 966 1 4676 198, Fax : 966 1 467 3662; amsamri@ksu.edu.sa

Team Organization 2: Lawrence Livermore National Laboratory
Principal Investigator of Team Organization 2: Dr. Arthur Rodgers, Lawrence Livermore National Laboratory, P.O. Box 808, Livermore, CA 94550, USA, Tel (925) 423-5018; Fax: (925) 423-4077; rodgers7@llnl.gov

Team Organization 3: Deschutes Signal Processing LLC
Principal Investigator of Team Organization 3: Dr. David B. Harris, Deschutes Signal Processing LLC, P.O. Box 231, Maupin, OR 97037, USA, Tel. (510) 331-8804; oregondsp@gmail.com

Abstract

The PIs propose a 3-year project to collect and process ground motion data from a newly deployed seismic array in the cratonic interior of Saudi Arabia. The array consists of nine, three-component sensors arranged in concentric circles, with an aperture of approximately 4 km. The PIs will develop and implement adaptive beamformers that take full advantage of polarization and slowness information to improve detection of regional phases in the Middle East. The performance of the three-component array will be compared to that of a co-located vertical component array and individual three-component stations sited in the Arabian shield. The primary deliverables from the project will be 3-4 years of continuous seismic data from the Saudi array, as well as quarterly progress reports and annual manuscripts submitted to the MRR.

INTRODUCTION

In the fall and winter of 2009, King Saud University deployed an array of three-component seismometers on the Arabian shield near the town of Ar Rayn, and near the GSN station RAYN (Figure 1). This array is located at a seismically quiet site on Precambrian crystalline bedrock. It presents an opportunity to investigate the potential for improving monitoring functions with signal detection and estimation methods that use arrays of three-component instruments. In addition, this is the first array intended for research in regional seismology to be deployed on the Arabian peninsula. It is at regional distance to many seismically active regions of interest throughout the Middle East, including the Red Sea rift, the Harrats of Saudi Arabia, the Zagros subduction zone, and the Turkish and Iranian plateaus. Along with three-component broadband seismometers of the Saudi Geologic Survey (Figure 1), this new array presents an unparalleled opportunity to characterize propagation throughout the region.

One of the themes that we intend to take up is the exploitation of predicted and measured structure in the signal and noise fields to improve detection and estimation algorithms. We intend to revisit adaptive beamforming methods in the attempt to reduce detection thresholds and make phase amplitude measurements at low signal-to-noise ratios. Adaptive beamforming methods were developed early (Capon et al., 1967; see Van Trees, 2002) to suppress noise with spatial structure or undesired signals in seismic data, but found their greatest use in radar, sonar, and acoustic applications. They operate by shaping the frequency-wavenumber (FK) response of array beamforming processors to suppress noise or undesired signals propagating in FK sectors (backazimuth and velocity) distinct from those of a desired signal.

A number of techniques are available to design adaptive beamformers, including the original minimum variance distortionless receiver (MVDR, also known as a maximum likelihood processor, Capon et al., 1968) that minimizes the output power of the beamformer subject to constraints that the desired signal, propagating with known direction and velocity parameters, is undistorted. Generally, adaptive beamformers default to conventional shift-and-sum beamformers when noise is spatially uncorrelated and spectrally flat.

Despite early research on adaptive beamforming in seismology in the 1960s and 1970s, they have not found wide acceptance, principally because their assumption of a plane-wave model for the desired signal is violated in practice, especially at high frequencies. Adaptive beamformers often reject desired signal as well as noise, as a consequence. In addition they originally were computationally expensive to implement (no longer a problem) and required complicated procedures to estimate noise structure. The last problem is largely dealt with now by using pre-defined noise models (Douglas, 1998; Selby, 2008), or so-called data-adaptive methods that do not require explicit knowledge of noise structure (e.g. Kobayashi, 1970; Frost, 1972).

In our research, we propose several innovations intended to generalize both conventional and adaptive beamformers to operate on three-component array data and to ameliorate the problems of signal loss:

1. Extension of conventional and minimum variance distortionless receiver beamformers to incorporate signal polarization constraints, making them suitable for an array of three-component sensors.
2. Extension of the approaches of Douglas (1998) and Selby (2008) that design adaptive beamformers using models of noise structure to exploit noise polarization as well as wavenumber structure. To do so, we will estimate the spatial-spectral-polarization structure of noise at the Ar Rayn array.
3. Extension of conventional and data-adaptive beamformers (e.g. Kobayashi, 1970; Frost, 1972) to use calibrated signal constraints in an effort to reduce signal cancellation. We think that signal loss can be mitigated by making the signal constraints used by these algorithms more realistic.

We emphasize that these signal processing methods are not an end in themselves, but rather a means to improving research and monitoring functions including event detection, location, discrimination and magnitude estimation. Consequently, we propose to examine how useful three-component array beamforming and phase amplitude estimation methods are in the context of these monitoring functions. We describe this goal in more detail in the next section.

While we expect this research on signal processing methods to be broadly applicable, we also recognize the unique position of the Ar Rayn array and intend that our analysis also will characterize propagation in this portion of the Middle East. We especially will have an opportunity to better characterize shear propagation in this region since we will have access to arrays of horizontal sensors.

OBJECTIVES AND OVERALL APPROACH

Our principal objective is to determine whether augmentation of an array of vertical sensors with horizontal components can provide significant improvements in the signal detection and estimation functions required for seismic monitoring. Our second objective is to determine whether arrays and arrays of three-component stations provide significant improvements specifically for this Arabian shield location, and to quantify the improvements in wave propagation characterization that can be obtained in this region by the new array.

Our overall approach to achieve these objectives will be to acquire statistics on phase detection and measurements of phase amplitudes on a large collection of events throughout the region with the array and surrounding stations, then assess implications for performance in detection, location, discrimination and magnitude (surrogate for yield) estimation functions. As described in the last section, we propose significant work on conventional and adaptive beamforming methods for detection and phase amplitude measurement (by improving observations of low SNR signals) on three-component array data. But we plan to go beyond algorithm development and apply these methods on large numbers of events to assess their potential contribution to monitoring functions.

For detection, our approach will be to operate vertical and three-component beams on the Ar Rayn array data with STA/LTA detectors to define event triggers to be compared with local

(KACST, SGS) and global catalogs, as well as with triggers by detectors operated on three-component stations closer to source regions of high seismicity. The latter would include stations of the LLNL-Kuwait broadband deployment and the SGS network close to the Zagros mountains, and SGS stations close to the Red Sea rift and the Harrats of western Saudi Arabia.

For discrimination and magnitude estimation, our approach will be to examine the scatter in populations of phase amplitude measurements made with beams of all types and individual station traces. We plan to make measurements of phase amplitudes with RBAP at LLNL on both beams and single station traces. We do not anticipate having populations of explosions in this region for evaluation of standard P/S discriminants, but we do anticipate being able to observe the scatter in discriminant measures for earthquakes. Our metric for success will be to observe whether the scatter is reduced for array beams as opposed to single stations.

In general we plan to examine detection and amplitude measurement performance on a variety of different station configurations: single vertical channel, single three-component sensor, array of verticals, array of three-component sensors. We plan to optimize processing for each configuration.

Finally, we intend to shed light on an old debate: is it better to have a good array located on crystalline basement, but possibly farther from a region of observed seismicity, or a more modest station located in a less optimal setting (e.g. on deep sediment cover), but much closer to the active region? This tradeoff can be examined in our study area by comparing the Ar Rayn array performance with the much closer Kuwait and SGS broadbands located along the Gulf (and on deep sediments) for the Zagros source region, and comparing western SGS stations with the Ar Rayn array for the Red Sea rift source region (as well as the Harrats of western Saudi Arabia).

BACKGROUND AND PREVIOUS WORK

In this section, we discuss previous work that we intend to draw upon in the execution of this proposed project.

Prior work on arrays of 3-component sensors

A significant amount of work was conducted in the mid-90s on algorithms for processing three-component array data [Wagner and Owens, 1993; Wagner, 1996; Wagner and Owens, 1996a; Wagner and Owens, 1996b]. Much of this was conducted with data from temporary three-component array deployments at Pinon Flats, California and Geyokcha, Turkmenistan.

Prior work on adaptive beamformers

As mentioned in the introduction, adaptive beamforming algorithms shape the frequency-wavenumber response of the array to suppress directional (or otherwise structured) noise while attempting to estimate an assumed plane-wave signal propagating with known

backazimuth and phase velocity. The methods are adaptive in the sense of adapting to the spatial and temporal characteristics of the noise; the spatial structure of the signal is assumed to be known. In all algorithms, the beam $b[n]$ is obtained as a sum of filtered, multichannel traces, e.g.:

$$b[n] = \sum_{k=-L}^{L} \mathbf{w}^T[k]\,\mathbf{x}[n-k] \tag{1}$$

Here the bold characters indicate multichannel quantities: the vector $\mathbf{x}[n]$ denotes the discretized waveform data observed by the array (n is the time index). The quantity $\mathbf{w}[n]$ represents a vector of impulse responses of filters applied to the array waveforms, here represented as finite impulse response filters with $2L+1$ coefficients. If the number of array channels is N, then the total number of scalar coefficients is $(2L+1)N$. Alternatively, the filters and beamforming operation may be represented in the frequency domain, replacing the indicated convolution with products of frequency-domain vector quantities.

Two general strategies for estimating the signal (defining the filter coefficients) have been applied. One finds a least-squares estimate of the signal [Burg, 1964], implementing a spatial Wiener filter when the noise is spatially uncorrelated. The more general least squares estimate (when noise is assumed to have spatial structure) has been used [Selby, 2008] to improve the traditional F detector [Blandford, 1974]. The other approach adapts the coefficients of the filters to minimize the output power of the array beam subject to fidelity constraints intended to pass the signal through the beamformer unchanged (MVDR [Capon, et al., 1968]). Although we intend to try the generalized F detector, we focus here on the MVDR beamformer since we are interested in measuring phase amplitudes in addition to detecting phases.

In the usual development of the MVDR beamformer, the data are considered to be shifted to align the incoming desired signals. The signal model then hypothesizes a common waveform on all channels of the array distributed with weights defined by the elements of the constraint vector $\mathbf{c}$:

$$\mathbf{x}[n] = s[n]\mathbf{c} \tag{2}$$

For an array of vertical sensors only, $\mathbf{c}$ is a vector of all ones. The filtering operation of the adaptive beamformer will pass the signal without distortion (i.e., $b[n] = s[n]$ if the filter impulse responses are constrained to satisfy:

$$\mathbf{c}^T\mathbf{w}[k] = \delta[k] \tag{3}$$

The filter coefficients are chosen to minimize the energy in the resulting beam

$$E = \sum_{n \in \Omega} (b[n])^2 \quad (4)$$

over some suitable training time interval Ω , subject to the constraints defined above. The classical approach [Capon et al., 1967] to designing the filter coefficients first estimates the covariance function for the noise over the training interval:

$$\mathbf{R}[k] = \underset{\square \in \Omega}{\mathbf{E}} \{ \mathbf{x}[n]\mathbf{x}^T[n+k] \} \quad (5)$$

then obtains the filter coefficients by solving normal equations (involving the covariance function) modified with Lagrange multipliers to satisfy the constraints. This approach is complicated, but simplified approximations exist that obtain the coefficients through a conjugate gradient solution [Kobayashi, 1970] or through a time-adaptive tracking algorithm [Frost, 1972] without the need for estimating the noise covariance. The Frost algorithm is especially suited to tracking non-stationary noise in a continuous beamforming operation.

The MVDR method is effective, but when the training interval includes the desired signal, undesirable signal cancellation usually results. Signal cancellation occurs because seismic phase arrivals do not satisfy the plane wave model very well, especially at high frequencies. Several approaches exist to minimize this problem. One (Douglas, 1998) uses a model for the noise, perhaps estimated over the long term, in place of adaptation to noise structure in a window surrounding the signal. Others involve estimating the noise structure in a pre-event window or over such a long window that the total noise energy dwarfs the signal energy and noise structure alone drives the optimization. The latter approach is suitable to situations where detection and signal amplitude estimation for very low-SNR events is the goal.

As we describe at greater length in the proposed research section, we plan several innovations to beamforming techniques: (1) extension of adaptive beamforming to incorporate polarization constraints on three-component array data, and (2) a different approach to mitigating signal loss: use of phase and amplitude calibrations to improve signal fidelity constraints.

Prior Work on FK Spectra of Ambient Noise

A significant advance in the study of ambient seismic noise took place in the 1960s with the advent of array seismology. Using frequency-wavenumber techniques it became possible to observe the phase velocity and backazimuth of diffuse, low-amplitude seismic noise, with better accuracy than was possible with polarization techniques (Backus et al., 1964; Backus, 1966; Toksoz and Lacoss, 1968; Lacoss et al., 1969; Capon, 1969a, 1969b; Haubrich and McCamy, 1969). This enabled body waves to be distinguished from surface waves, and particular sources of microseisms to be accurately located. A review of these efforts is given in Koper et al. (2010) and the focus here is on describing the previous work of the PIs, which will be most applicable to the proposed work.

Two IMS arrays in particular have been closely analyzed by the PIs: the Chiang Mai array in

Thailand (CMAR) and the Yellowknife array in Canada (YKA). These arrays are both larger than the Saudi array and so sensitive to slightly longer period energy, however the principles of the analysis are the same. In Koper & de Foy (2008), around 1,000 samples of noise over a 10-year period were processed with f-k techniques. Similar results were found using the maximum likelihood technique of Capon (1969a) and a time-domain packing method based on phase stack weighted beams. At frequencies lower than about 1.5 Hz, the noise was organized into Lg waves from the southwest and the east, and steeply arriving body wave energy (PKP) with indeterminate backazimuth. In Koper et al. (2009) over 6,000 windows of noise from YKA were processed. Results were consistent between conventional FK spectral estimation and the maximum likelihood technique. At periods of 2-3 s several distinct sources of naturally occurring seismic noise were identified: Rg waves from the Great Slave Lake; Lg waves from the Atlantic, Pacific, and Arctic Oceans; and teleseismic P waves from the north Pacific and equatorial mid-Atlantic regions. A year-long comparison of noise properties from 18 IMS arrays in given in Koper et al. (2010).

Prior work on characterization of propagation and phase amplitudes

Broadband (0.5-16 Hz) regional phase amplitudes and their ratios are essential for identification of low yield nuclear explosion discrimination (e.g. Taylor et al., 1989; Walter et al., 1995; Hartse et al., 1997; Rodger s and Walter, 2002), magnitude (Mayeda and Walter, 1996; Mayeda et al., 2003) and yield estimates (Nuttli, 1986; Hansen et al., 1990; Patton, 2001; Murphy et al., 2009). This was clearly illustrating with the recent nuclear tests in North Korea (Koper et al., 2008; Hong et al., 2008; Hong and Rhee, 2009; Fisk et al., 2009). However, the frequency-dependent amplitudes of regional phases are strongly impacted by attenuation and crustal waveguide effects. In the past these effects have been characterized by mapping regional phase propagation characteristics (Molnar and Oliver, 1969; Ni and Barazangi, 1983). Studies in the Middle East found inefficient (attenuated) propagation of Sn in the Turkish-Iranian Plateau and Lg blockage for paths crossing the Zagros Mountians (Kadinsky-Cade at al., 1989; Rodgers et al., 1997; Mellors et al., 1999; Al-Damegh et al., 2004). Paths crossing the Arabian Platform generally show clear high-frequency Sn and Lg, while paths crossing the Arabian Shield have attenuated Sn and exceptionally strong Lg (Mellors et al., 1999; Al-Damegh et al., 2004). Recently, Pasyanos et al. (2009a, 2009b) used quantitative amplitude measurements and simultaneous inversion to estimate source, and path-dependent attenuation and site effects for broadband regional phase amplitudes. The formulation is based on the Magnitude-Distance Amplitude Correction (Walter and Taylor, 2002) using quantitative physical model of regional phase amplitudes. Figure 7 shows the resulting models for crust and mantle attenuation quality factors for compressional and shear waves. These maps can be used to estimate the expected regional phase amplitudes.

For station Ar-Rayn in central Saudi Arabia we expect Sn and Lg to propagate moderately efficiently from events in Turkey and the Zagros Mountains. Observations of Lg propagating from the Zagros region to central Arabia can be complex due to the deep sedimentary cover. These paths tend to show long duration short-period surface waves and Lg (Al-Amri et al., 2008). However, for events farther away in higher elevations of Turkish-Iranian Plateau we

expect regional shear wave phases to be weak, due to low mantle Q and crustal waveguide heterogeneity. For paths crossing the Arabian Shield (e.g., from events in the Gulf of Aqaba, Red Sea, Horn of Africa) Sn should be very weak due to low mantle Q_S. This quantitative documentation of regional phase behavior illustrates the need for three-component array signal-processing to enhance signal-to-noise levels in the region. Furthermore, as events get smaller and farther away, single levels will decrease in addition to path attenuation effects.

THE AR RAYN ARRAY

The department of Geology of King Saud University has established a small-aperture (~ 3.5 km) three-component seismic array in central Saudi Arabia at a hard rock site on the Arabian Shield. The facility consists of well-constructed vaults in hard rock outcrops in a region that has very low background noise. The deployed equipment consists of a broadband three-component sensor (STS-2) as the center element, and eight short-period three-component sensors at the outlying elements (Figure 2).

Details of installation

Great care was taken to site the stations on Precambrian outcrops. Figure 3 shows a representative station site (AR25). Note that the station is sited adjacent to a rock outcrop where it was possible to excavate a vault into contact with undisturbed Precambrian bedrock. The inside dimension of the vault is 1.6 meters square and 2 meters deep (Figure 2). At the bottom a 1.4 meter by 1.4 meter concrete pier, 20 cm thick, was poured directly on bedrock. This dimension affords a 10 cm separation between the pier and the walls of the vault for noise isolation. The walls themselves are composed of two shells, a concrete block wall on the outside, with foam filling the voids of the blocks for thermal isolation, and a 20 cm inside wall poured of solid concrete. Neither of the walls contain any steel reinforcement to prevent possible noise contributed to the motion of the mass. The top of the vault is covered by a double door with 10 cm of foam for thermal isolation. The walls and top of the vaults are flush with the ground surface to minimize wind noise. The 80 watt solar panel is mounted close to the ground surface also to minimize wind noise that would be transmitted into the vault if a mast mounting had been used.

The short-period instruments are Kinemetrics SS-1 one Hz free period Ranger seismometers. Three are arranged in a three-component configuration as shown in Figure 3 (right). The data are acquired by Quanterra Q330 data loggers and the data are stored on Belar 44 data storage devices with thirty-two gigabytes of flash memory. The sampling rate presently is 100 samples per second for each channel. The single broadband sensor at the center of the array (AR00) is a Streckheisen STS-2. Otherwise the configuration of this installation is the same as the short-period stations.

Examples of event data and processing

We now show two examples of data recorded during the initial two weeks of operation of the array. The first example is a teleseismic observation of an m_b 5.3 earthquake in the vicinity of

Greece (USGS preliminary hypocenter 38.425N 22.044E, depth 10 km) that occurred on January 22, 2010 at 00:46:57.5 GMT. Figure 4 (top) displays the P waveforms from the arrays vertical short-period sensors, aligned and superimposed. The data have been filtered into the 1-3 Hz band. The back-azimuth (-63.4 degrees) and phase velocity (10.2) values estimated from the FK spectrum computed from this P window were used to align the signals for a coherence analysis. The bottom of Figure 4 shows the correlation values of all 21 distinct pairs of signals plotted as a function of sensor separation. The correlation values are quite high, as is expected for a low-frequency (~ 1 Hz) teleseismic P phase observed across a 4 kilometer aperture. Nonetheless, the high correlation values indicate desirable uniformity of vault installation, coupling to bedrock and instrumentation.

An interesting observation of a local event is shown in Figures 5 and 6. This is a local magnitude 2.3 (KACST catalog) event which occurred approximately 260 kilometers NNE of the array. Only the Lg phase is clear in the data (top trace, Figure 5) filtered into the 0.8 to 3 Hz band. There is a hint of a P phase approximately 30 seconds before the Lg signal, but nothing that can be reliably picked for an arrival time. Higher frequency filter bands do not improve the signal to noise ratio in this case. A wideband (1-3 Hz) FK spectrum of the Lg arrival (Figure 6) provides a usable back-azimuth and a phase velocity confirming the identity of the Lg phase. The measured Lg back-azimuth and an assumed phase velocity of 8 km/sec can be used to search for the P phase arrival. The middle trace of Figure 5 shows the conventional P beam, in which the (probable) Pn phase now is clearly visible.

Still greater processing gain can be obtained for the P phase by combining beamforming and polarization filtering. The third trace in the figure shows a polarized beam obtained by forming separate beams on the vertical, north and east components of the array, then rotating the resulting three-component beam consistent onto the polarization vector of Pn for this event (back-azimuth 29.5 degrees, angle of incidence 39 degrees). The angle of incidence used assumes a medium velocity of 5 kilometers per second. This processing approach roughly doubles the signal-to-noise ratio of the incident P wave, enhancing our ability to pick and identify this phase.

PROPOSED RESEARCH

Data Collection

The proposed study will use data principally from the new Ar Rayn array described in section previously. In addition we plan to obtain data from the permanent broadband network operated by the Saudi Geologic Survey (SGS) to measure regional phase amplitudes and improve propagation models for the Middle East. Figure 1 shows the distribution of stations operated by the SGS. Data will be obtained by the King Saud University team for regional events (distances less than 2000 km). We also will have access to two broadband stations currently operating in Kuwait (under a joint project between LLNL and the Kuwait Institute of Scientific Research) and the Global Seismic Network (GSN) station UOSS operated by IRIS-IDA (Figure 1). Data will be archived at KSU and the University of Utah, and loaded into the LLNL Seismic Research Database for subsequent phase amplitude measurements.

An example of Ar Rayn observations of an event in the Zagros subduction zone, the most seismically active area within regional distance of the Ar Rayn array, is shown in Figure 8. According to the NEIC bulletin this is a mb 4.4 event located at 32.36N 48.33E which occurred at 09:34:24.9 GMT on January 17, 2010. A more detailed plot of the three-component waveforms recorded at one station (AR11) is shown in Figure y, with theoretical arrival times indicated for the four principal regional phases. The Pn time assumes an upper mantle P velocity of 8.0 km/sec and a crustal-leg offset of 5 seconds and appears to be an excellent prediction. The Pg time is estimated using a group velocity of 6.0 km/sec and appears to be early. The Sn time was predicted using 4.5 km/sec upper mantle S velocity and a 9-second crustal leg offset. The Lg time corresponds to a group velocity of 3.5 km/sec.

Investigation of Noise Structure

This work will be carried out by University of Utah personnel and can be split into three subtasks. First is characterization of the noise by means of coherence and correlation analysis. Both of these quantities will be computed as a function of frequency and station separation. The coherence map in particular is important since it will be used as input to an adaptive beamformer (i.e., Selby 2008). It is expected that this function will vary considerable over time, perhaps with hourly and seasonal periods, and this variation will be quantified and modeled. As a second subtask, existing algorithms for FK-style noise analysis will be applied to the vertical component channels of the Ar-Rayn array. At the time the award is made, all available data will be processed in this manner. The geographical, temporal, and modal variability of the vertical component noise will be assessed, documented, and compared with previous results for 18 IMS arrays from the study of Koper et al. (2010). As a third subtask, the FK analysis will be applied to the horizontal components of the array. We will also develop and implement a method of analyzing the radial and transverse components of the ambient noise. For each slowness vector in a reasonable grid, the horizontal spectra will be rotated appropriately to generate a measure of radial and transverse energy. The transverse component of ambient noise is rarely studied, and the uncommon three-component properties of the Ar-rayn array will allow us to have this capability.

Signal Processing: Detection and Parameter Estimation

We plan to extend adaptive beamforming algorithms to include polarization constraints. Such modifications are straightforward for linearly polarized signals. For a P wave incoming with incidence angle ϕ and backazimuth θ, the constraint vector of equations 2 and 3 is modified to:

$$\mathbf{c} = \begin{bmatrix} \mathbf{e} \\ \mathbf{e} \\ \vdots \\ \mathbf{e} \end{bmatrix}; \qquad \mathbf{e} = \begin{bmatrix} \cos\phi \\ -\sin\phi\cos\theta \\ -\sin\phi\sin\theta \end{bmatrix} \tag{6}$$

where the corresponding vector of signal observations from the array is modified to replace each vertical with the three-component set:

$$\mathbf{x}[n] = \begin{bmatrix} \mathbf{x_1}[n] \\ \mathbf{x_2}[n] \\ \vdots \\ \mathbf{x}_N[n] \end{bmatrix}; \qquad \mathbf{x}_i[n] = \begin{bmatrix} x_{zi}[n] \\ x_{ni}[n] \\ x_{ei}[n] \end{bmatrix} \tag{7}$$

An example of this approach is shown in the top four traces of Figure 10. At left is a conventional P beam for the event signals shown in Figures 8 and 9, using only the vertical components of the array, and beneath it is an adaptive beam. At right are the corresponding conventional and adaptive beams using the full three-component array, and the constraint vector of equation (6). Here the conventional three-component beam is defined by:

$$b[n] = \frac{\mathbf{c}^T \mathbf{x}[n]}{\mathbf{c}^T \mathbf{c}} \tag{8}$$

and is essentially the same algorithm as the one used to produce the bottom trace of Figure 5.

The objective in this example is to obtain a better estimate of incident P waves, suppressing everything else (shear waves included). Note that the three-component beams reduce the shear phases more effectively than their vertical-component counterparts. It also is apparent that the adaptive beams reduce the shear phase more than the conventional beams. Comparing the adaptive beams to their non-adaptive counterparts, though, shows that some P signal loss occurs, and, in fact, is worse for the three-component beam than the vertical channel beam.

A more substantial improvement to beamformers may result from calibrating signal fidelity constraints. Since signal loss is a consequence of the fact that real seismic signals are only approximately plane waves, loss may be reduced if the fidelity constraints represent signal structure more realistically. This might be achieved by a calibration approach wherein the amplitude (and, potentially, phase) structure of signals across an array are estimated from prior event observations. A particularly simple calibration obtains the constraint vector $\mathbf{c}$ as the principal eigenvector of a wideband covariance matrix

$$\mathbf{R} = \sum_n \mathbf{x}[n]\mathbf{x}^T[n] \tag{9}$$

calculated for the particular target phase of a calibration event. The covariance matrix can be averaged over as many calibration events as are available for a given source-receiver path. As described, this type of calibration will correct amplitudes in the constraint vector. If the data are filtered into narrow frequency bands and the signal vectors $\mathbf{x}[n]$ are replaced by their complex analytic representations, then this calibration will correct constraint phase as well as amplitude across the array.

The bottom four traces of Figure 10 show the result of adding calibration to the beamforming algorithms (conventional and adaptive, vertical-only and three-component). For both the vertical and three-component adaptive beams, the addition of calibration has ameliorated P signal loss. We propose to examine systematically the gains in performance that calibration in beamforming may provide, extending the simple results shown here to frequency-dependent amplitude and phase calibrations.

Comparison of Detection and Estimation Performance of the Ar Rayn Array and Broadband Stations in Kuwait, the UAE and Eastern and Northern Saudi Arabia

The metrics of beamforming performance relevant to monitoring issues are the improvements in phase detection and parameter (e.g. amplitude, arrival time) estimation that underpin event detection, discrimination, location and magnitude or yield estimation. Consequently, we propose to apply the algorithms we develop to phase detection and parameter estimation on a large number of events at regional distances from the Ar Rayn array. The basic performance metrics we propose to evaluate will be the probability (expressed as frequency) of phase detection as a function of false alarm rate, and the bias and variance of phase arrival time, back-azimuth, phase velocity and amplitude measurements (which we hope our processing techniques will reduce). We propose to evaluate these metrics on four station configurations: single vertical channel, single three-component station, array of vertical components only, array of three-component sensors. We further propose to optimize the signal processing, to the best of our ability, for each configuration to make the comparison fair. Our intent is to characterize the increase in performance afforded by each increase in complexity of station configuration.

To make these proposed comparisons, we need to perform detection processing of months of continuous data and acquire large numbers (several hundred at least) of event observations for parameter estimation.

To estimate detection performance, we propose to implement beams (conventional, adaptive, calibrated as appropriate) with power detectors to cover the area surrounding the Ar Rayn array at regional distances. To grade detection performance, we propose to reconcile detections made with this processor against available local/regional (e.g. KACST, KISR) and global catalogs and against detections made with simpler stations close to highly-active source regions (LLNL-Kuwait and eastern SGS for the Zagros subduction zone, western SGS for the Red Sea rift and the Harrats (volcanic areas) of Saudi Arabia).

To evaluate parameter estimation performance, we propose to make FK, phase amplitude and phase arrival-time measurements for a large collection of regional events. We plan to make these measurements on single channels and the various array beams that we have been discussing. We propose to do so efficiently using the RBAP and KBALAP software systems at LLNL on event segments that we have extracted from continuous data archived at KSU, LLNL and the University of Utah. For example, the RBAP (Regional Body—Wave Amplitude Processor) implements the standardized NNSA Knowledge Base algorithm for measuring

regional phase and noise amplitudes and saves them to the LLNL Database for easy retrieval, selection and analysis. KBALAP (Knowledge Base Automated Location Assessment and Prioritization) implements FK measurements. Both RBAP and KBALAP archive measurements efficiently to a database for subsequent analysis, saving extensive measurement metadata.

We do not propose to evaluate discriminant performance directly, because we do not anticipate having access to large numbers of explosions in the region. Nonetheless, some judgment about discrimination performance can be developed from the variances of parameter estimate populations for earthquakes alone (the higher the variance, the worse discriminant performance can be expected to be). We propose to contrast population variances for the different station configurations and for a range of distances from regions of high seismicity (Zagros, Red Sea).

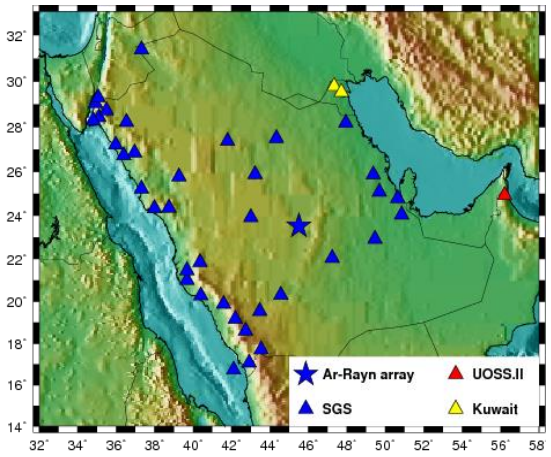

Figure 1 Stations from which data will be acquired in this proposed project . The three-component array at Ar Rayn and the large number of broadband three-component stations across the Arabian Peninsula make will make this data set unique for studying propagation in the region and for determining the special capabilities of three-component

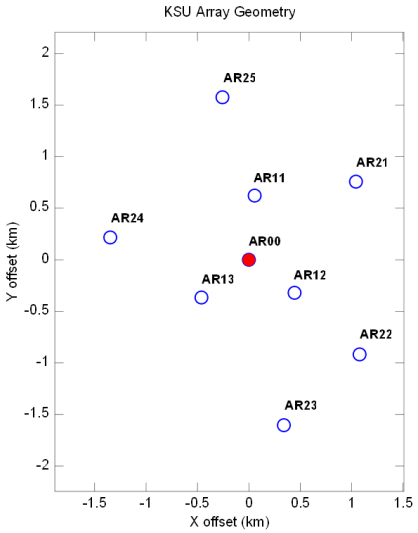

Figure 2 The King Saud University seismic array has a broadband (STS-2) three-component sensor at its central location (filled circle) surrounded by two rings of three-component short-period (Ranger) sensors.

Figure 3 Station sites (left) were chosen for Precambrian bedrock contact. Typical vault installation (right) shows the concrete pier poured on bedrock.

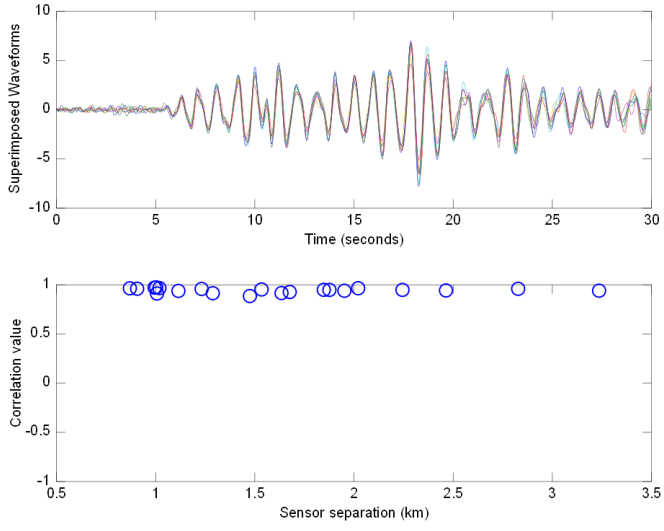

Figure 4 Coherence of the teleseismic P phase at the array is high, demonstrating uniformity of installation and instrumentation. At top, the teleseismic P waves of an event in Greece are superimposed to show the domain of calculation of signal correlation. At the bottom, the 21 correlation coefficients between unique pairs of sensors are shown plotted as a function of sensor separation. The P phase is relatively narrowband, with most of its energy just above 1 Hz.

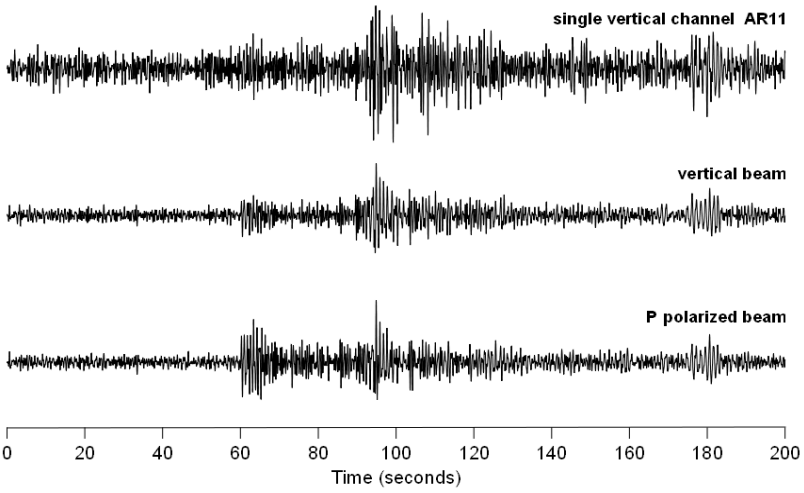

Figure 5 Beamforming greatly enhances our ability to interpret the P phase of this small central Arabian event. The top trace is the waveform from a single vertical sensor of the array filtered into the 0.8 to 3 Hz band. The second trace is the conventional beam made with the vertical elements of the array, using the Lg backazimuth (29.5 degrees) and an assumed Pn phase velocity of 8 km/sec. The third trace is the beam formed from all seven three-component traces, assuming polarization consistent with Pn (P medium velocity of 5 km/sec; incidence angle of 39 degrees).

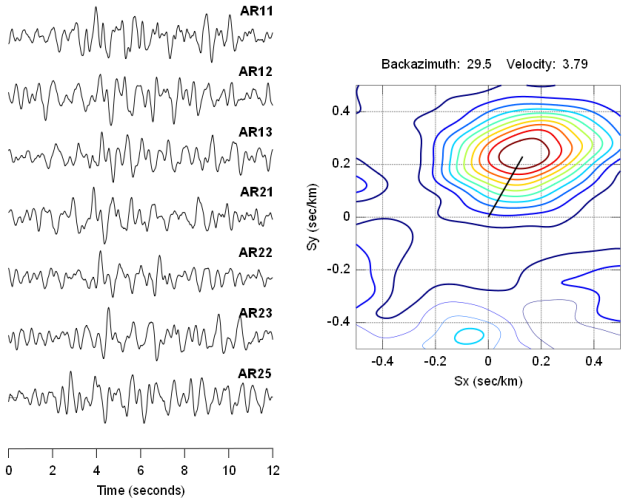

Figure 6 The Lg phase window (left) of the small central Arabian event shown in Figure 4. The FK spectrum of the Lg phase (right) provided the backazimuth and phase velocity used in the beams of Figure 4.

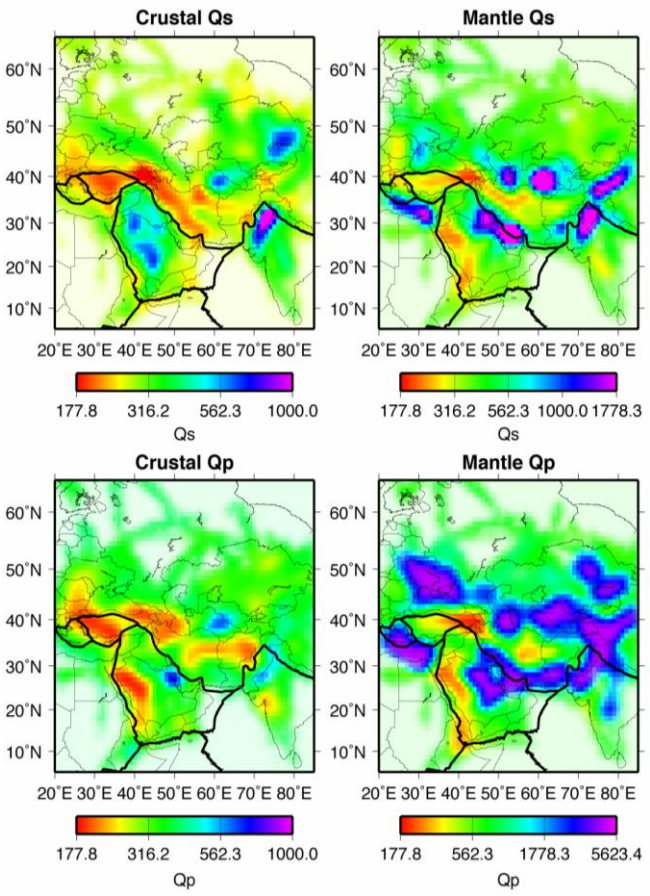

Figure 7 Qs and Qp for crust and upper mantle in the study region determined from path measurements indicated in Figure 6 (Pasyanos et al., 2009a,b).

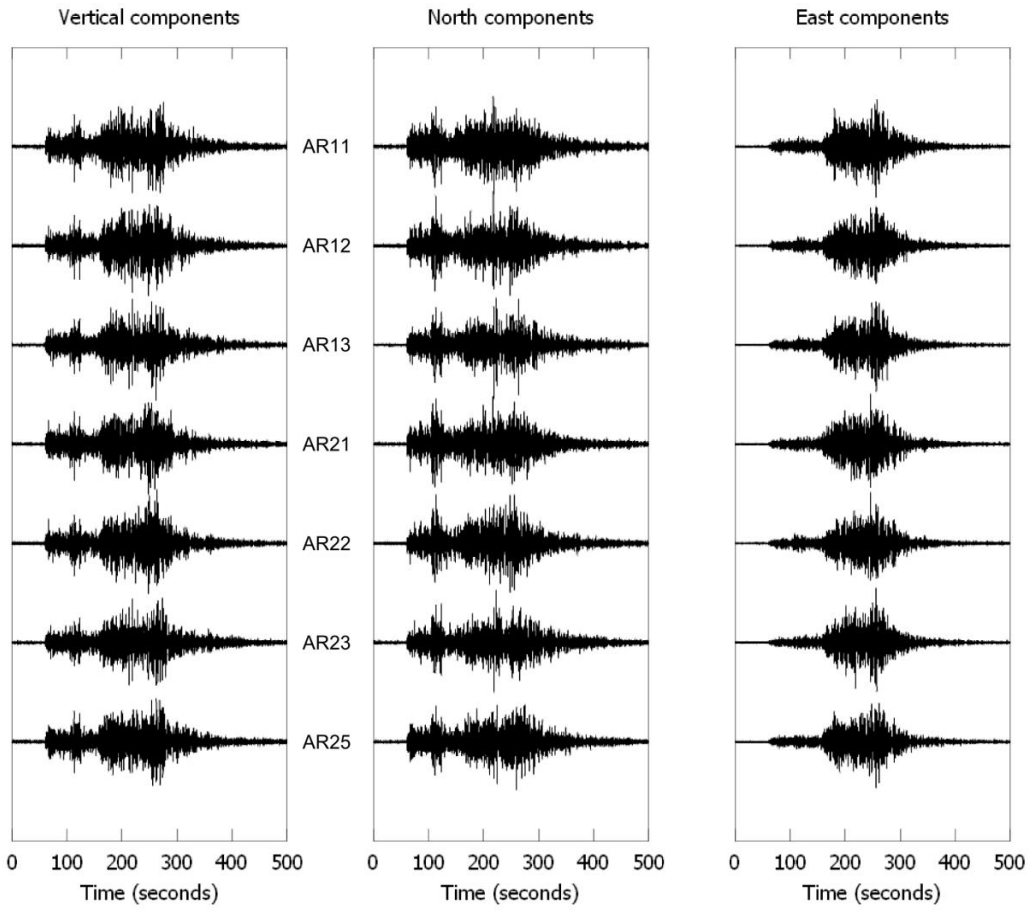

Figure 8 Three-component array data for an event in the Zagros mountains (32.36N 48.33E). This event is used in subsequent discussions of beamforming approaches.

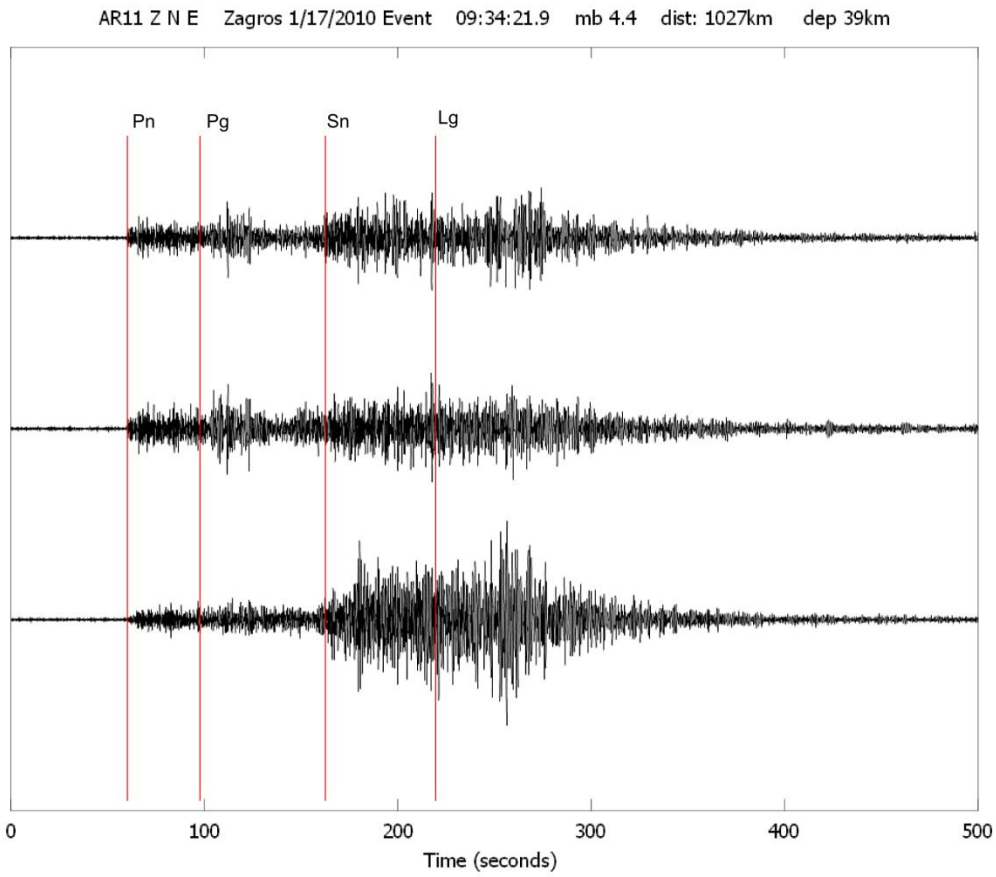

Figure 9 Detail of the Zagros earthquake for one array station (AR11), including approximate regional phase arrival times. The vertical, north and east channels are shown on the top, middle and bottom of the plot, respectively. This event is close to due north (15.9 degrees backazimuth), so that the east channel is approximately transverse. P phases have the expected polarization, but the Sn time window has significant transverse energy.

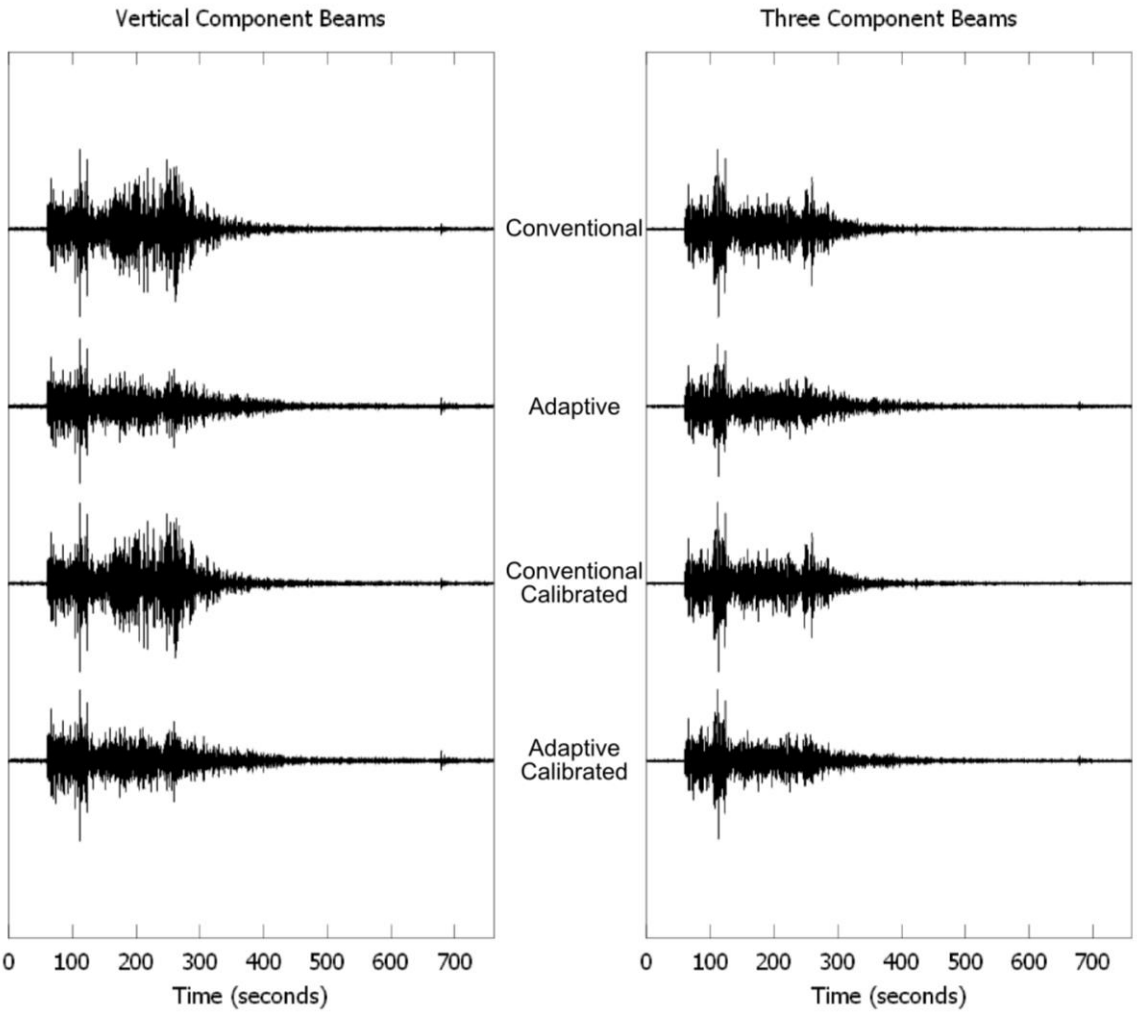

Figure 10 Comparison of beams steered for compressional waves shows that adaptive beamforming, use of three-component data and use of P amplitude calibrations all contribute to suppressing shear waves.

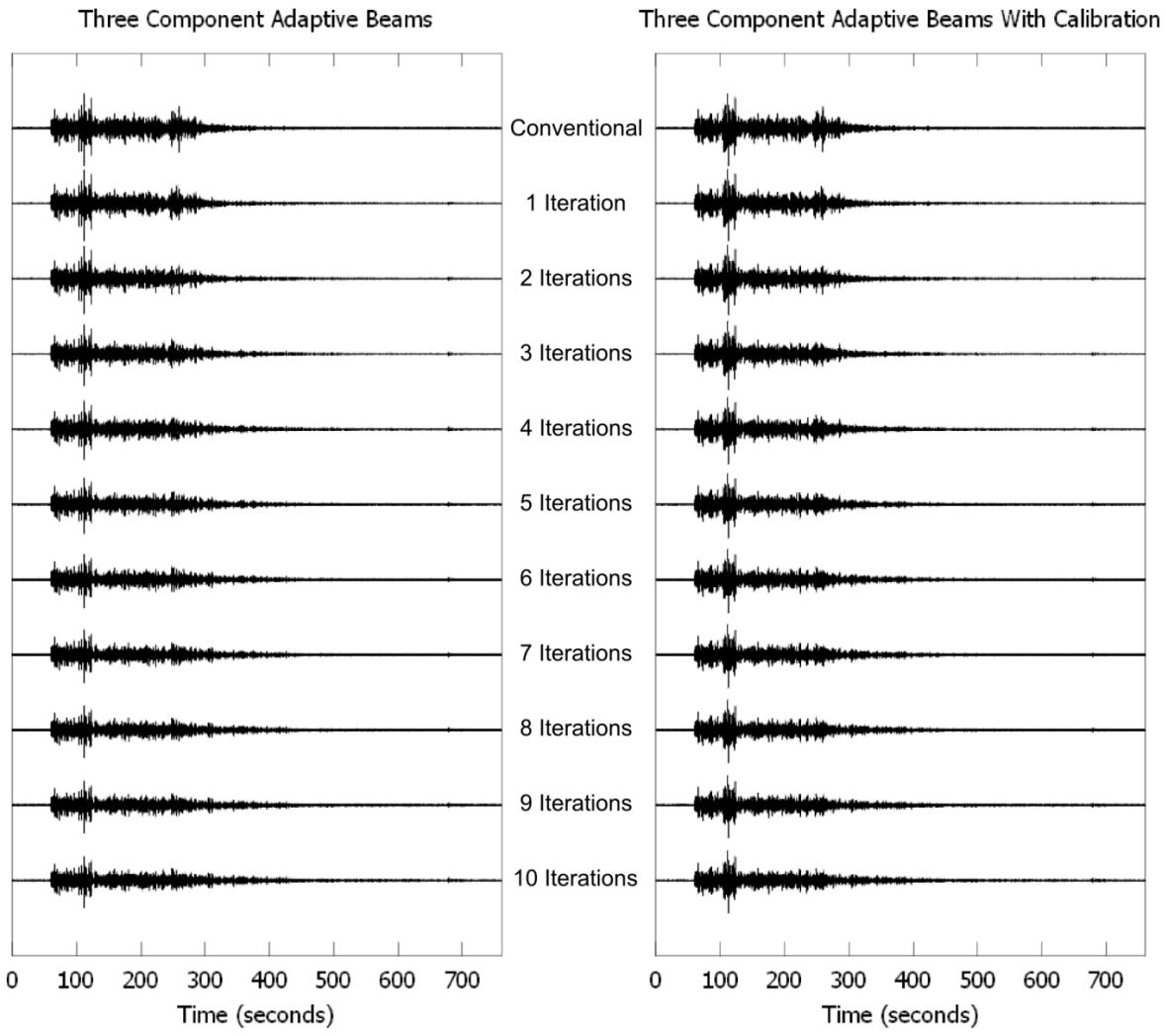

Figure 11 Calibration of amplitudes in adaptive beamforming constraint vectors reduces signal loss. Both panels show beams with the weights obtained from successive iterations of the conjugate gradient algorithm used to estimate the adaptive beam weights with Kobayashi's algorithm. Note that P signal loss is significant (left), but reduced (i.e. P amplitudes increased) with calibration (right).

REFERENCES

Al-Amri, A. M. S., A. Rodgers and T. Al-Khalifah (2008). Improving Seismic Hazard Assessment in Saudi Arabia, *Arabian J. Geosciences, 1*, 1-15.

Al-Damegh K, Sandvol E, Al-Lazki A, Barazangi M (2004). Regional wave propagation (Sn and Lg) and Pn attenuation in the Arabian plate and surrounding regions, *Geophy. J. Int., 157*, 775–795.

Backus, M. M. (1966). Teleseismic signal extraction*, Proc. R. Soc. A. 290*, 343–367.

Backus, M., J. Burg, D. Baldwin, and E. Bryan (1964). Wide-band extraction of mantle P waves from ambient noise, *Geophysics 39*, 672–692.

Blandford, R. R. (1974). An automatic event detector at the Tonto forest observatory, *Geophysics, 39*, 633–643.

Burg, J. P. (1964). Three-dimensional filtering with an array of seismometers, *Geophysics 29*, 693-713.

Capon, J. R. Greenfield, and R. Kolker (1967). Multidimensional maximum-likelihood processing of a large aperture seismic array, *Proc. IEEE*, *55*, 192-211.

Capon, J. (1969a). High-resolution frequency-wavenumber spectrum analysis, *Proc. IEEE 57*, 1408–1418.

Capon, J. (1969b). Investigation of long-period noise at the Large Aperture Seismic Array, *J. Geophys. Res. 74*, 3182–3194.

Douglas, A. (1998). Making the most of the recordings from short-period seismometer arrays, *Bull. Seismol. Soc. Am., 88*, 1155–1170.

Fisk, M., S. Taylor, W. Walter, and G. Randall (2009). Seismic Event Discrimination Using Two-Dimensional Grids of Regional P/S Spectral Ratios: Applications to Novaya Zemlya and the Korean Peninsula in Proceedings of MRR2009 Monitoring Research Review: Ground-Based Nuclear Explosion Monitoring Technologies, LA-UR-09-05276.

Frost, O. L. (1972). An algorithm for linearly constrained adaptive array processing, *Proc. IEEE*, *60(8),* 926 – 935.

Hansen, R. A., F. Ringdal, and P. G. Richards (1990). The stability of rms Lg measurements and their potential for accurate estimation of the yields of Soviet underground nuclear explosions, *Bull. Seismo. Soc. Am., 80*, 2106-2126.

Harris, D. B. (2006). Subspace Detectors: Theory. Lawrence Livermore National Laboratory Report UCRL-TR-222758.

Harris, D. B. and T. Kvaerna (2010). Superresolution with seismic arrays using empirical matched field processing, in press, *Geophys. J. Inter.*

Hartse, H. E., S. R. Taylor, W. S. Scott, and G. E. Randall (1997). A preliminary study of regional seismic discrimination in central Asia with emphasis in western China*, Bull. Seismol. Soc. Am., 87*, 551–568.

Haubrich, R. A., and K. McCamy (1969). Microseisms: Coastal and pelagic sources, *Rev. Geophys. 7*, 539–571.

Hong, T.-K., C.-E. Baag, H. Choi and D.-H. Sheen (2008). Regional phase observations of the October 9 2006 underground nuclear explosion in North Korea and the influence of crustal structure on regional phases, *J. Geophys. Res., 113*, B03305, doi:10.1029/2007JB004950.

Hong, T.-K., and J. Rhee (2009). Regional source scaling of the 9 October 2006 underground nuclear explosion in North Korea, *Bull. Seismol. Soc. Amer., 99*, 2523-2540, doi:10.1785/0120080007.

Kadinsky-Cade, K., M. Barazangi, J. Oliver, and B. Isacks (1981). Lateral variations in high-frequency seismic wave propagation at regional distances across the Turkish and Iranian plateaus, *J. Geophys. Res. 86,* 9377-9396.

Kobayashi, H. (1970). Iterative synthesis methods for a seismic array processor, *IEEE Trans. On Geoscience Electronics*, *GE-8(3),* 169-178.

Koper, K, R. B. Herrmann and H. M. Benz (2008). Overview of open seismic data from the North Korean event of 9 October, 2006, *Seism. Res. Lett., 79 (2),* 178-185, doi:10.1785/gssrl.79.2.178

Koper, K.D. and B. de Foy (2008). Seasonal anisotropy in short-period seismic noise recorded in South Asia, *Bull. Seism. Soc. Am., 98*, 3033-3045, 2008.

Koper, K.D., B. de Foy, and H.M. Benz (2009). Composition and variation of noise recorded at the Yellowknife Seismic Array, 1991-2007, *J. Geophys. Res., 114*, B10310, doi:10.1029/2009JB006307.

Koper, K.D., K. Seats, and H.M. Benz (2010). On the composition of Earth's short period seismic noise field, *Bull. Seism. Soc. Am., 100*, 606-617.

Lacoss, R. T., E. Kelly, and M. N. Toksóz (1969). Estimation of seismic noise structure using arrays, *Geophysics 34*, 21–38.

Mayeda, K., and W. R. Walter (1996). Moment, energy, stress drop, and source spectra of western United States earthquakes from regional coda envelopes, *J. Geophys. Res. 101*, 11,195-11,208.

Mayeda, K., A. Hofstetter, J. L. O'Boyle, and W. R. Walter (2003). Stable and transportable regional magnitudes based on coda-derived moment-rate spectra, *Bull. Seismol. Soc. Am. 93*, 224-239.

Mellors, R. J., V. E. Camp, F. L. Vernon, A. M. S. Al-Amri, and A. A. Gharib (1999). Regional waveform propagation in the Arabian Peninsula, *J. Geophys. Res., 105(B3*), 6305.

Molnar, P. and J. Oliver (1969). Lateral variations of attenuation in the upper mantle and discontinuities in the lithosphere*, J. Geophys. Res. 74*, 2648-2682.

Murphy, K. R., K. Mayeda, and W. R. Walter (2009). Lg-Coda Methods Applied to Nevada Test Site Events: Spectral Peaking and Yield Estimation, *Bull. Seism. Soc. Am., 99*, 441-448.

Ni, J. and M. Barazangi (1983). High-frequency seismic wave propagation beneath the Indian shield, Himalayan arc, Tibetan plateau and the surrounding regions: high uppermost mantle velocities and efficient Sn propagation beneath Tibet, *Geophys. J. R. Astr. Soc. 72*, 665-.

Nuttli, O. W. (1986). Yield estimates of Nevada Test Site explosions obtained from seismic Lg waves*, J. Geophys. Res. 91*, 2137-2151.

Pasyanos, M., E. Matzel, W.. Walter, and A. Rodgers (2009a). Broad-band Lg attenuation modeling in the Middle East, *Geophys. J. Int., 177*, 1166-1176.

Pasyanos, M.E., W.R. Walter, and E.M. Matzel (2009b). A simultaneous multi-phase approach to determine P-wave and S-wave attenuation of the crust and upper mantle, *Bull. Seism. Soc. Amer. 99-6,* DOI: 10.1785/0120090061.

Pasyanos, M.E., and W.R. Walter (2009c). Improvements to regional explosion identification using attenuation models of the lithosphere, *Geophys. Res. Lett. 36*, L14304, doi:10.1029/2009GL038505.

Patton, H. J. (2001). Regional magnitude scaling, transportability, and Ms:mb discrimination at small magnitudes, *Pure Appl. Geophys., 158*, 1951-2015.

Rodgers, A., J. Ni and T. Hearn (1997). Propagation characteristics of short-period Sn and Lg in the Middle East, *Bull. Seism. Soc. Amer., 87*, 396-413.

Rodgers, A. and W. Walter (2002). Seismic discrimination of the May 11, 1998 Indian nuclear test with short-period regional data from station NIL (Nilore, Pakistan), *Pure appl. geophys., 159*, 679-700.

Selby, N. D. (2008). Application of a generalized F detector at a seismometer array. *Bull. Seismol. Soc. Am.*, *98(5),* pp. 2469–2481.

Taylor, S. R., M. D. Denny, E. S. Vergino, and R. E. Glaser (1989). Regional discrimination between NTS explosions and western U.S. earthquakes, *Bull. Seismol. Soc. Am., 79*, 1142–1176.

Toksoz, M. N., and R. T. Lacoss (1968). Microseism: Mode structure and sources, *Science 159*, 872–873.

Van Trees, H. L. (2002). *Optimum Array Processing: Detection Estimation and Modulation Theory*, Part IV, John Wiley & Sons.

Wagner, G. S. (1996). Resolving diversely polarized, superimposed signals in three-component seismic array data, *Geophys. Res. Lett.*, *23(14),* 1837–1840, doi:10.1029/96GL01599.

Wagner, G. S. and T. J. Owens (1993). Broadband bearing-time records of three-component seismic array data and their application to the study of local earthquake coda, *Geophy. Res. Lett. 20(7)*, 1823-1826.

Wagner, G. S. and T. J. Owens (1996a). Broadband eigen-analysis for three-component seismic array data. *IEEE Trans. on Signal Processing, 43(7),* 1738-1741.

Wagner, G. S. and T. J. Owens (1996b). Signal detection using multichannel seismic data. *Bull. Seismol. Soc. Amer.*, *86(*1a), 221-231.

Walter, W. R., K. Mayeda, and H. J. Patton (1995). Phase and spectral ratio discrimination between NTS earthquakes and explosions, part 1: Emipirical observations, *Bull. Seismol. Soc. Am. 85*, 1050–1067.

Walter, W.R. and S.R. Taylor (2001). A revised magnitude and distance amplitude correction (MDAC2) procedure for regional seismic discriminants: theory and testing at NTS, Lawrence Livermore National Laboratory, UCRL-ID-146882.